Journal of Marine Systems 129 (2014) 234–247

Contents lists available at ScienceDirect

Journal of Marine Systems

journal homepage: www.elsevier.com/locate/jmarsys

On thermohaline structure and circulation of the Western Large Aral Sea from 2009 to 2011: Observations and modeling

A.S. Izhitskiy [a,*], P.O. Zavialov [a], E. Roget [b], H.-P. Huang [c], A.K. Kurbaniyazov [d,e]

[a] P.P. Shirshov Institute of Oceanology, 36, Nakhimovskiy Prospect Ave., Moscow 117997, Russia
[b] University of Girona, PII. Campus Montilivi, Girona 17071, Catalonia, Spain
[c] Arizona State University, Tempe, AZ 85287-6106, USA
[d] Ahmet Yassaui International Kazakh-Turkish University, Turkestan, Kazakhstan
[e] Qaraqalpaq State University, Nukus, Uzbekistan

ARTICLE INFO

Article history:
Received 19 April 2013
Received in revised form 24 June 2013
Accepted 27 June 2013
Available online 4 July 2013

Keywords:
Aral Sea
Circulation
Thermohaline structure

ABSTRACT

The shrinkage of the Aral Sea in the second half of the past century has significantly affected the hydrophysical regime of the lake. The objective of this paper is to report on a hydrological structure and circulation of the today's Aral Sea based on both direct field observations and modeling results. We focus on the results of three field surveys to the Aral Sea which took place in the period from 2009 to 2011. In addition, series of numerical experiments using Princeton Ocean Model adapted to the Aral Sea was undertaken to investigate the contributions from bathymetry and water stratification in the formation of the basin scale circulation. The hydrological structure of the Aral's western basin in autumn season exhibited a three-layered pattern with two local salinity maxima, separated by a fresher intermediate layer. According to direct observations, water circulation in the surface layer has anti-cyclonic character, while circulation in the bottom layer has cyclonic sign under the predominant northerly winds. The simulation experiments demonstrated clearly that the main cause of the anti-cyclonic circulation in the surface layer of the lake is the "asymmetric" bathymetry with broad shallow area along the eastern coast and relatively steep and deep western slope. However, strong stratification is a necessary condition for the formation of the cyclonic circulation gyre in the bottom layer.

1. Introduction

Until 1960, the Aral Sea, a terminal lake in Central Asia, was the World's fourth largest inland water body by area. Mainly because of intensive water diversion from the Amu-Darya and Syr-Darya rivers for irrigation, the Aral Sea began to shrink dramatically in 1960. In comparison with pre-desiccation state, to the date of this writing, the overall level drop was about 26 m. Nowadays, the Aral Sea has lost more than 90% of its volume (Zavialov et al., 2012). The shrinkage resulted in profound changes of the lake's ecosystem and desertification of the surrounding areas. The ecological crisis of the Aral Sea has attracted attention of mass media and international scientific community. Moreover, the significance of the ongoing changes of the Aral Sea is not limited to the applied, regional aspects. The lake can be thought of as a "natural laboratory", where the evolution of a large inland water body under anthropogenic intervention through diversions of the river runoff can be investigated. Such an investigation could be also instructive with respect to other similarly exposed regions all over the World.

The Aral Sea was covered by data relatively well in the times of the former USSR. However, during the period of the most rapid changes of the Aral Sea hydrological system, i.e., the 1990s, the in situ observations in the lake were extremely sparse. The reason was the well-known political and economic troubles following the collapse of the USSR, as well as the complete cessation of the navigation in the Aral Sea at advanced stages of desiccation. This resulted in a practically total lack of data about many basic characteristics of the rapidly changing Aral Sea environment at the beginning of the new millennium. Most works published after the early 1990s were confined to either modeling or remote sensing (e.g., Ginzburg et al., 2002). In 2002, the Shirshov Institute of Oceanology of the Russian Academy of Sciences (SIORAS) launched a long-term program of field research and monitoring of the Aral Sea. The field observations are conducted in collaboration with a number of other institutions in Russia and Central Asia's states of Uzbekistan and Kazakhstan.

The objective of this article is to report on a hydrological regime and circulation of the today's Aral Sea based on both direct field observations and some modeling results. The paper is centered on the results of the 3 latest field surveys of SIORAS to the Aral Sea which took place in August, 2009, September, 2010 and November, 2011. Similar data collected in the surveys since 2002 through 2008 have been published previously (e.g., Zavialov, 2005, 2009), and in this paper we recall them only briefly,

* Corresponding author. Tel.: +7 9031197766.
E-mail address: izh@ocean.ru (A.S. Izhitskiy).

0924-7963/$ – see front matter © 2013 Elsevier B.V. All rights reserved.
http://dx.doi.org/10.1016/j.jmarsys.2013.06.013

mainly focusing on the results of 2009, 2010 and 2011 presented here for the first time.

The paper also reports on numerical model simulations of the Aral Sea circulation. The properties of basin-scale circulation gyres in major lakes have been subject of a number of previous studies. For example, Schwab and Beletsky (2003) investigated relative importance of different mechanisms to explain the large-scale gyres in Lake Michigan and found that wind stress curl and the baroclinic effects were the dominant factors, but the topographic effects were also significant. The effects of bathymetry on circulation patterns in lakes have been addressed in early works by Shtokman (1953). Pickett and Bermick (1977) studied Lake Ontario during the stratified season and reported a circulation consisting of a major counterclockwise gyre complemented with a smaller clockwise gyre in the northern part of the lake. In the case of Great American Lakes (whose geographic and morphological settings are in some respects similar to those of the Aral Sea), Beletsky et al. (1999) argued that the observed cyclonic circulation pattern was associated with the vorticity of the wind stress field. However, smaller lakes tend to manifest two-gyre rather than a single gyre circulation patterns. For example, double gyre circulations were observed in the Lake Tahoe (e.g., Rueda et al., 2005; Strub and Powell, 1986). A combination of an anticlockwise gyre and a weaker clockwise gyre has also been reported for the Lake Kinneret (Marti and Imberger, 2008). Shimizu et al. (2007) studied the Lake Biwa during the stratified period and identified anticyclonic sub-basin scale gyres. Beletsky et al. (2006) concluded that in general, the density effects added to the wind action led to a more complex circulation pattern in lakes.

In the present paper, we investigate the circulation of today's hyperhaline, highly stratified Aral Sea and attempt to quantify the underlying mechanisms based on in situ measurements as well as numerical modeling. Information about geographical and physical conditions of the Aral Sea as well as the historical background of the problem are summarized in Section 2. Details of the field campaigns and the model experiments are given in Section 3. The thermal and salinity structures across the main lobe of the Aral Sea are presented and analyzed in the Section 4. Investigation of water circulation based on observations is analyzed in Section 5 and numerical modeling results are presented in Section 6. Conclusions are drawn in Section 7.

2. Geographic settings of the lake

The Aral Sea in its original, pre-desiccation state was a brackish lake whose salinity varied only slightly around 10 g/kg. The minimum values were mainly associated with river mouth areas, while the highest were distributed in the deepest western part of the basin. The seasonal cycling of salinity was largely insignificant (Kosarev, 1975). In contrast with the salinity values, the temperature demonstrated strong spatial and temporal variability. High seasonal range of SST (about 25 °C) and steep thermocline with maximum vertical gradients up to 1 °C/m were characteristics for the lake in the summer season

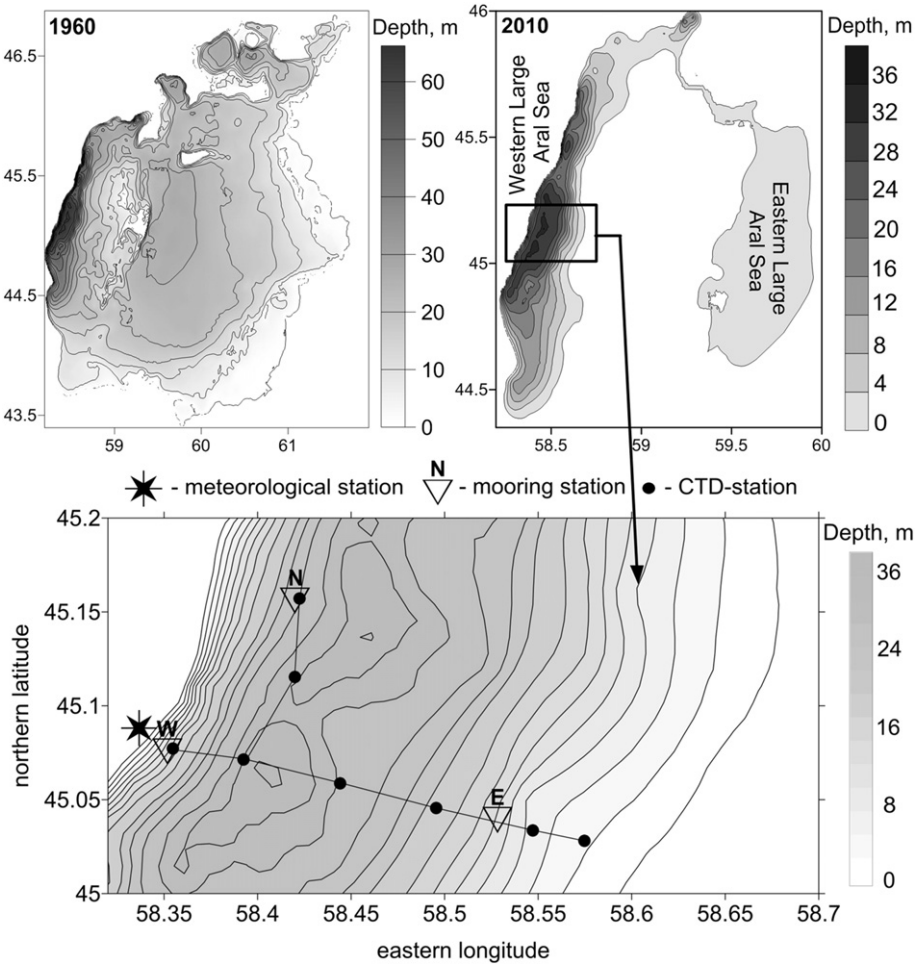

Fig. 1. The Aral Sea bathymetry for 1960 and for 2010, the Eastern Large Aral Sea is shown schematically (upper panel). Schematic illustrating the locations of 6 CTD-stations on the annual cross-section, two additional CTD-stations north, 3 mooring stations and meteorological station (lower panel). The positions were retained during every field survey.

Table 1
Field surveys and measurements used in this study.

Survey	CTD measurements	Mooring stations
August, 2009	*SBE 19plus SeaCat* 10 stations	"E": 19–23 August, 2009 velocity and pressure at 2 m depth — *Nortek Aquadopp*; bottom velocity — *SeaHorse*; "W": 18–23 August, 2009 surface velocity — *SonTek Argonaut-MD*; bottom velocity — *SeaHorse*; sea level variability — *pressure gauge at bottom*
September, 2010	*SBE 19plus SeaCat* 11 stations	"E": 16–19 September, 2010 velocity and pressure at 2 m depth — *Nortek Aquadopp*; bottom velocity — *SeaHorse*; "W": 14–19 September, 2010 surface velocity — *SonTek Argonaut-MD*; bottom velocity — *SeaHorse*; sea level variability — *pressure gauge at bottom* "N": 17–19 September, 2010 bottom velocity — *SeaHorse*; sea level variability — *pressure gauge at bottom*
November, 2011	*SBE 19plus SeaCat* 3 stations	"W": 3–5 November, 2011 days velocity and pressure at 2 m depth — *Nortek Aquadopp*; bottom velocity — *SeaHorse*

(Bortnik and Chistyaeva, 1990). Therefore, the vertical stratification of the pre-desiccation Aral Sea was mainly controlled by the temperature regime rather than salinity. Cooling of the upper layer of the lake in autumn caused convection movement throughout the water column down to the bottom. This factor provided for seasonal mixing of the water column and prevented the formation of pronounced density stratification. These features of hydrological structure were also typical for the Aral Sea during the early stages of the desiccation (Bortnik and Chistyaeva, 1990).

The thermohaline structure of the Aral Sea at the present stage of advanced desiccation is much different from the pattern observed in the middle of the last century. Starting from 1960, a continuous increase of salinity has been observed. The salinity growth was essentially uniform across different parts of the lake until the late 1990s, when the Large Aral Sea divided into two basins, i.e., the Western Large Aral Sea and the Eastern Large Aral Sea, connected through a narrow strait formed due to intensive bottom erosion during the shrinking period (Roget et al., 2009). Since then, salinity growth in the broad and shallow eastern basin became more intense than in the relatively deep and less extensive western basin. The differences in TS-characteristics of eastern and western basins created strong horizontal salinity gradients. Also, the penetration of much saltier water from the eastern basin to the west basin through the connecting strait resulted in strong salinity and, hence, density stratification in the western basin of the Large Aral Sea. As observed in surveys to the Aral Sea conducted by SIORAS since 2002, two archetypes of hydrological structure of the western basin in

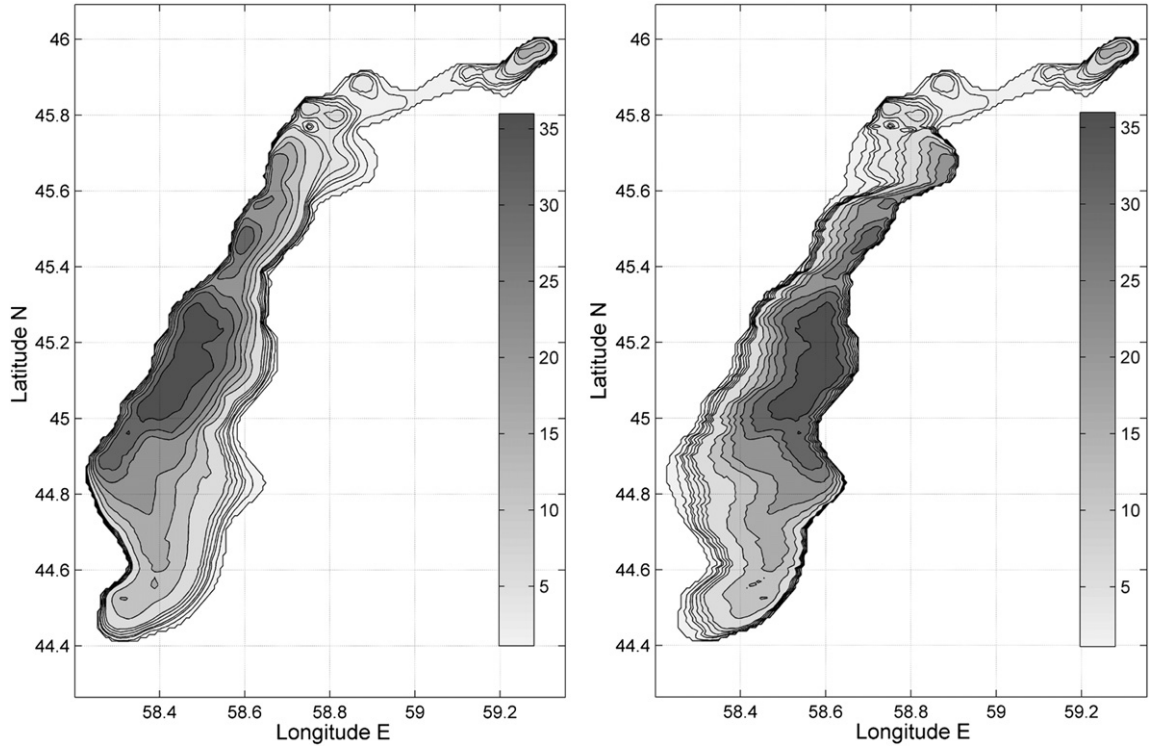

Fig. 2. Bathymetry of the western basin used in the model simulations: real bathymetry as of 2010 (left panel), inverted bathymetry (right panel).

fall and summer seasons were persistent through the last decade. The first type is characterized by "two-layered" structure with salinity minimum in the upper mixed layer, followed by steep halocline and salinity maximum in the bottom layer. The other type of stratification exhibits the "three-layered" pattern with two salinity maxima, one in the upper mixed layer and one in the bottom layer, separated by a layer of fresher water. In this case, vertical stability is maintained by steep thermocline. It has been hypothesized that these features of hydrological structure of the western basin were determined by two mechanisms, sometimes termed as *convective* and *advective* (e.g. Zavialov, 2005; Zavialov et al., 2012). The convective mechanism provides for salinity growth in the upper mixed layer by means of intense evaporation from the surface of the lake in the warm season. In this case, the water column retains stable density stratification until the beginning of the autumn cooling and subsequent development of the vertical convection. On the other hand, the local salinity maximum in the bottom layer is connected with the advective mechanism, which implies the water inflow from the eastern basin through the connecting strait. Direct measurements of 2004 yielded estimate of this inflow at about 1500 m^3/s (Zavialov, 2005). The much saltier and denser waters from the east fill the bottom layer of the western basin, providing for extremely stable density stratification. The TS-analysis based on CTD-measurements obtained in autumn 2002 showed that 9 to 11% of water in the bottom layer of the western basin had originated from the eastern basin (Zavialov, 2005). The resulting high vertical gradients of density largely suppress the autumn/winter convection. The frequent features of the present day Aral Sea such as the temperature inversions, anoxia and hydrogen sulfide contamination in the bottom layer are manifestations of reduced mixing. In contrast with the convective mechanism, the advective one exhibits strong interannual variability (Zavialov et al., 2012).

The circulation of the pre-desiccation Aral Sea had not been thoroughly explored because of relatively small number of direct measurements. However, even the early researchers pointed out that the lake's mean circulation pattern appeared to have the anticyclonic direction (Berg, 1908; Zhdanko, 1940). This is rather unusual, given that the neighboring inland seas, such as the Caspian Sea, the Black Sea and the Azov Sea, belonging to the same latitudinal belt and exposed to similar predominant winds, all maintain cyclonic character of their large-scale circulation. The early researchers of the Aral Sea hypothesized that this peculiar feature of the Aral Sea's surface circulation resulted from the impact of river inflows (Berg, 1908; Zhdanko, 1940). This hypothesis was based on simplified calculations such as the geostrophic method, as well as analyses of plankton concentration as a tracer for the currents. Later on, basing on theoretical works by V.B. Shtokman, A.I. Simonov attributed the anticyclonic sign of Aral Sea's surface circulation to a combined effect of the predominant northerly winds inhomogeneously distributed over the basin, and the lake's bathymetry (Shtokman, 1953; Simonov, 1954). Furthermore, some model results showed that the surface circulation can switch to cyclonic under the conditions of southerly winds (Bortnik and Chistyaeva, 1990). In addition, the baroclinic motions of denser waters from relatively shallow eastern part of the lake to the western trench have been documented even before the onset of the desiccation (Simonov, 1962).

Recent studies (e.g. Zavialov, 2005) pointed out that the sign of circulation gyre in the Aral Sea's surface layer did not change during the desiccation. Indeed, despite the drastic changes in the bathymetry and geometry of the sea, the basin-scale surface circulation in the Western Large Aral Sea retained the anticyclonic character. In this paper, we report new data supporting this notion and discuss possible mechanisms responsible for the observed character of the present day circulation. During the field campaigns carried out during 3 consecutive years, measurements of current velocity and wind stress were performed on site at high temporal resolution. This allowed analyzing the short-time response of the lake to the wind variability. On the other hand, because the mean wind conditions during the field

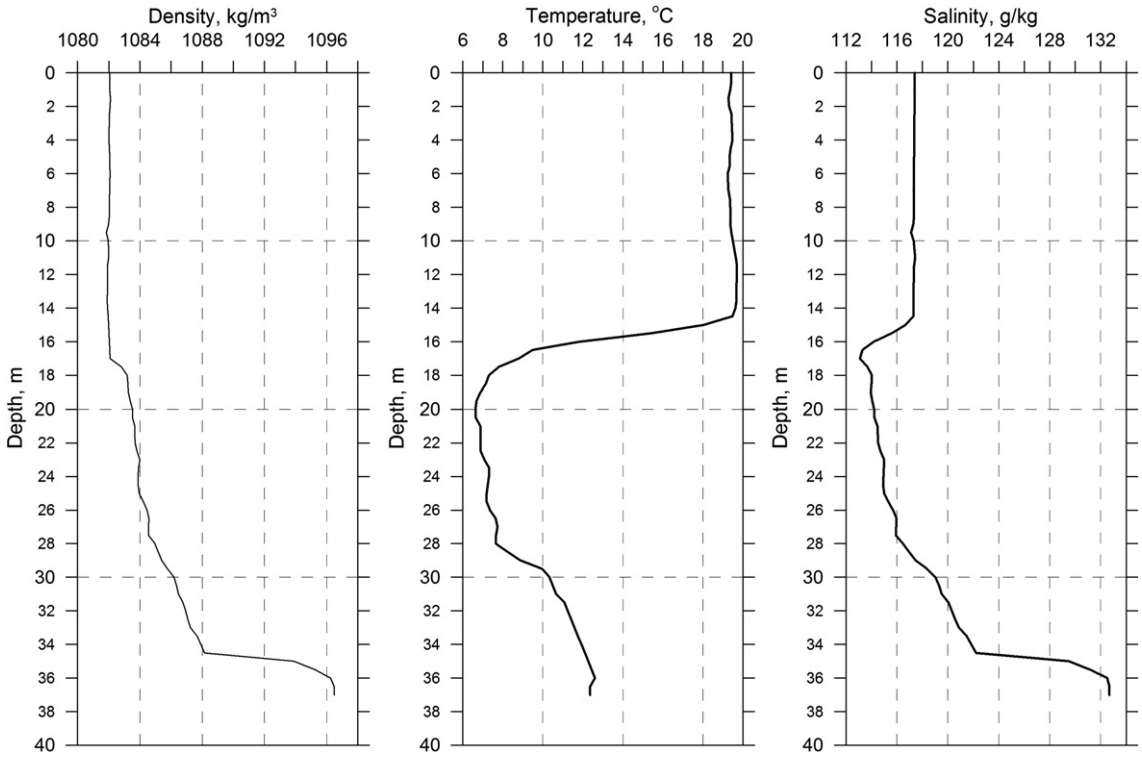

Fig. 3. Vertical profile of density, temperature and salinity used in the simulation, as inferred from CTD measurements in September, 2010.

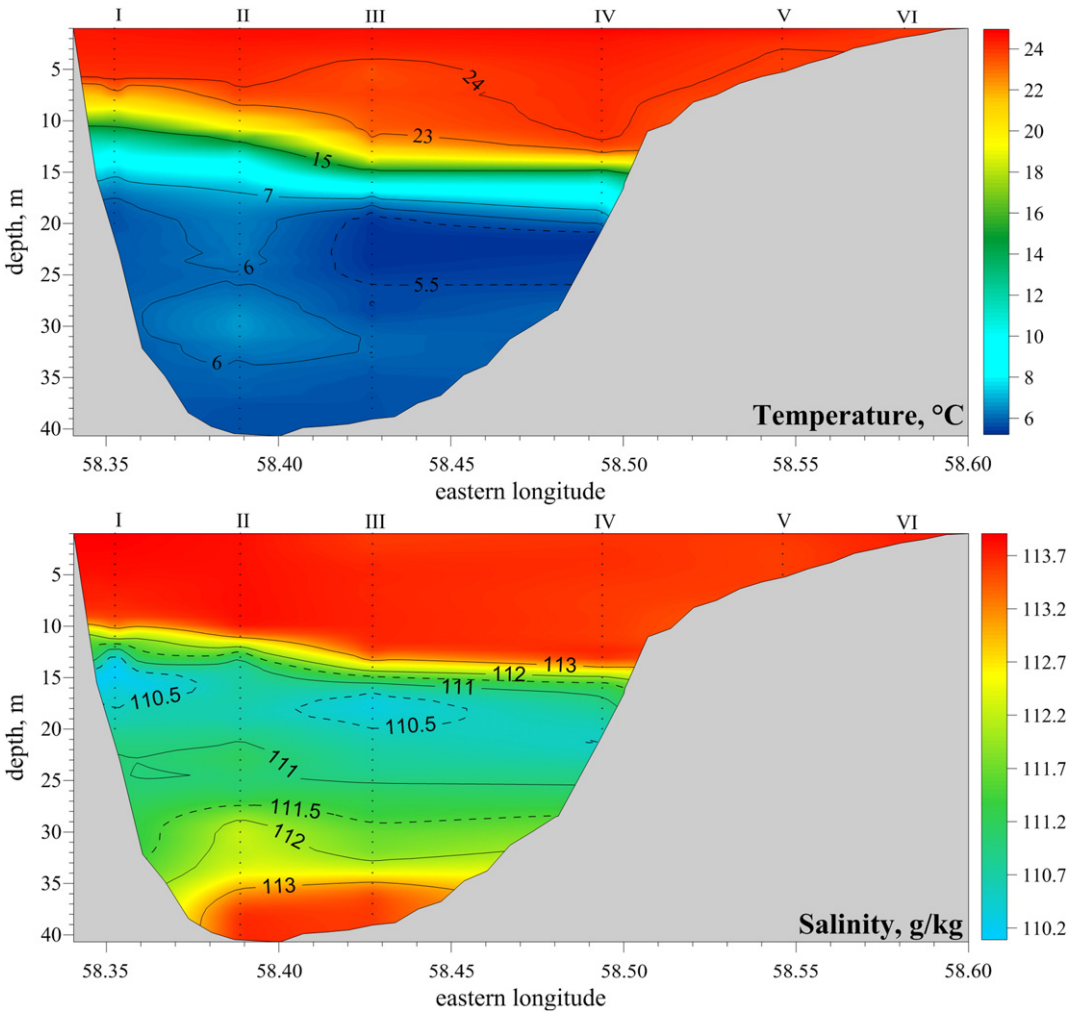

Fig. 4. Vertical distribution of temperature (°C, upper panel) and salinity (g/kg, lower panel) along zonal cross-section of the western basin in August, 2009.

experiments were rather close to the climatic regime (Bortnik and Chistyaeva, 1990) the recorded data can also be used to validate the results of numerical model forced by climatic winds.

3. Data and methods

3.1. Observations

The research area is situated in the deepest portion of the western basin of the Aral Sea (Fig. 1). Each of the field surveys (August, 2009, September, 2010 and November, 2011) included CTD-profiling, deployment of mooring stations with current meters and pressure gauges, and water sampling. A summary of the measurements is given in Table 1.

Surface-to-bottom CTD-profiling was performed at 4 Hz sampling rate at regular section across the western basin (Fig. 1), using *SBE 19plus SeaCat* profiler. As known, general problem with interpreting CTD data collected from the Aral Sea is linked with the salt composition of the water, which is significantly different from the ocean water. In consequence, the relation between the electric conductivity and salinity is also different. Therefore, we applied the following procedure to infer the salinity from the original CTD data. First, the true salinities of the collected water samples were obtained chemically in laboratory through "dry residue" method. Then, the corresponding "pseudo salinity" values S_{ctd}, i.e., those computed through the standard oceanic relation, were extracted from the CTD data, and linear regression between the laboratory salinity and CTD-derived pseudo salinity values was constructed. The linear relation obtained thereby was then used to convert the entire set of CTD data to the "true" salinity. This conversion was done on an individual basis for each cruise. As an example, we give here the following regression based on chemically analyzed water samples collected in September, 2010:

$$S_{real} = 1.107 * S_{ctd} + 18.48. \quad (1)$$

Mooring stations equipped with current meters, one near the surface (depth 3–5 m) and one in the near bottom layer (depth 20–22 m) at each mooring, as well as pressure gauge at the bottom, were deployed at the locations shown in Fig. 1. Mooring station "W" was installed at the western slope of the basin, while the station "E" was positioned at the eastern slope. Additionally, in September, 2010, a northern mooring station "N" was placed a 9 km to the north. Each of the moorings remained in operation for 4–5 days following the installation, collecting the data every 1 min. Also, a portable automatic meteorological station, continuously recording the wind speed and other principal meteorological parameters at 10 min sampling rate, was installed near the mooring site "W". The time series of the sea level variability, surface and bottom currents obtained at the moorings were then filtered with 10-min wide moving window. The lagged correlations between these parameters and wind stress were calculated to investigate the relations between the wind stress as a forcing factor and the water circulation as a basin response. Finally, the absolute

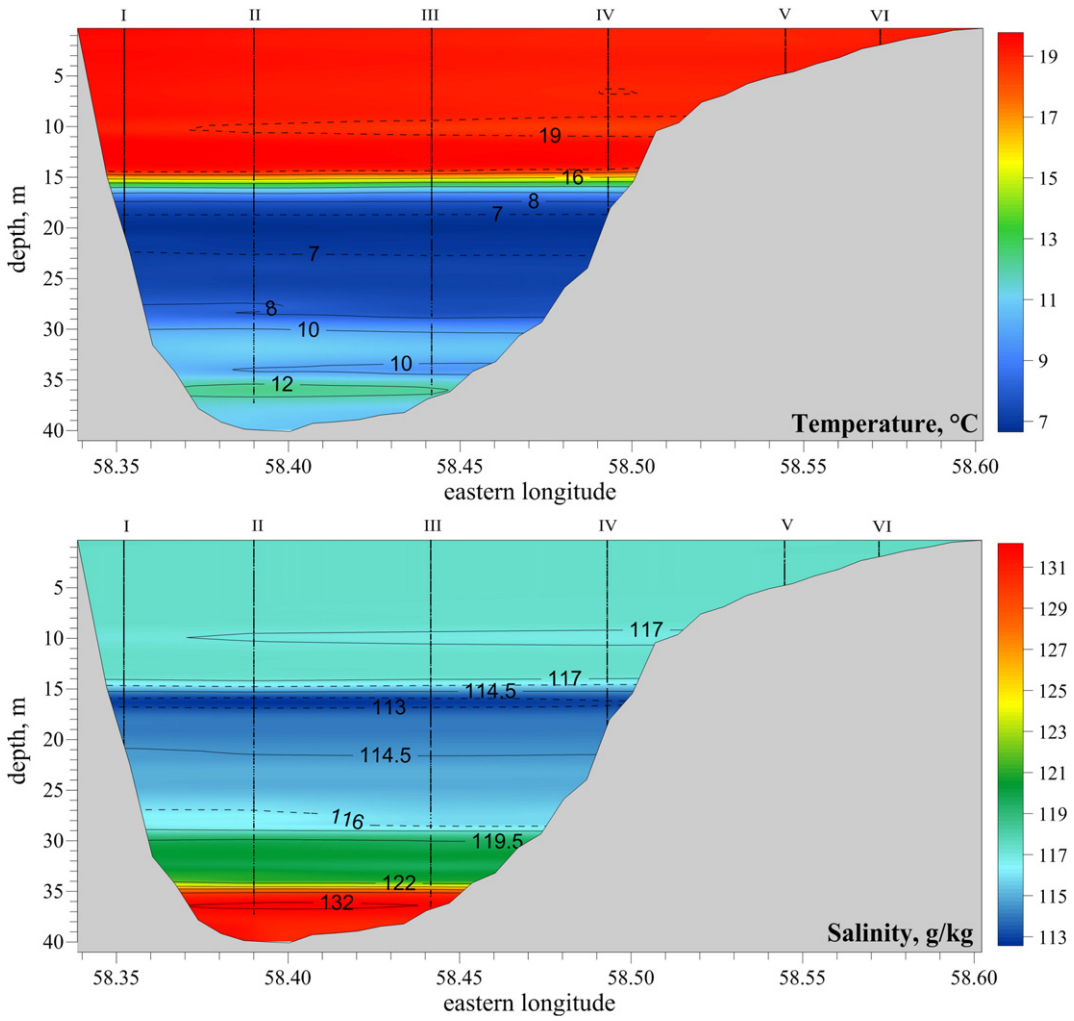

Fig. 5. Vertical distribution of temperature (°C, upper panel) and salinity (g/kg, lower panel) along zonal cross-section of the western basin. September, 2010.

elevation of the Aral Sea surface above the ocean level was determined through direct geodesic leveling using a nearby triangulation beacon located at the western bank of the western basin.

3.2. Model specifics

Apart from analysis of the in situ observations, we used the obtained data to implement model simulations in order to investigate the origin of the anticyclonic character of water circulation in the surface layer of the lake under the predominant northeasterly winds. A series of numerical experiments where performed by using the 3D Princeton Ocean Model (POM) (Mellor, 1992) adapted to the Aral Sea was undertaken at the University of Girona. The bathymetry of the western basin of the Aral Sea (Fig. 2, left panel) was digitized in a grid with 211 nodes along NS direction with a resolution of 967.02 m and 173 nodes along the EW direction with a resolution of 538.67 m. For the vertical coordinate a total of 17 equidistant sigma levels were considered. Maximum depth of the numerical model of the lake in 2010 was 39 m and the mean of 4 m.

The duration of each model experiment was 12 days and the results presented correspond to the mean values computed between the days 9 and 12. The model was forced by a constant and spatially uniform 3 m/s NE wind, which is in agreement with the climatic wind conditions over the Aral Sea region (Bortnik and Chistyaeva, 1990). Wind stresses were computed according to $\tau = \rho_a C_D V^2$, the drag coefficient C_D being parameterized according to Hasselman (1988). Similar approach is considered for the bottom stress where the drag coefficient was calculated in order to fit the velocities at the first grid points nearest the bottom to the law of the wall, considering a bottom roughness of 0.01 m. Zero normal velocities were used as the lateral boundary conditions. For all simulations the heat flux at all the boundaries was set to zero.

As mentioned above, the bathymetry is thought to be one of the main factors determining the sign of water circulation in the Aral Sea. Despite the enormous morphometric changes accompanying the desiccation, the bathymetry of the lake retained its principal pattern, also characteristic for the pre-desiccation state: the western slope is very steep, while the eastern slope is much gentler. It has been hypothesized by (Simonov, 1954) that such an asymmetry could be one of the factors determining the anticyclonic sign of the circulation gyre. To verify this statement, we also repeat model experiments with the bathymetry inverted with respect to the longitudinal axis of the basin (Fig. 2, right panel) and look at the changes which the inversion produces in the circulation regime.

For each experiment, either stratified or non-stratified initial conditions were imposed. In the former case, the "real" stratification inferred from CTD measurements of 2010 were used (Fig. 3). The specific equation of state (i.e., the relation between temperature, salinity and density) recently obtained by (Gertman and Zavialov, 2011) for the present-day Aral Sea was used in the model instead of the oceanic equation of state

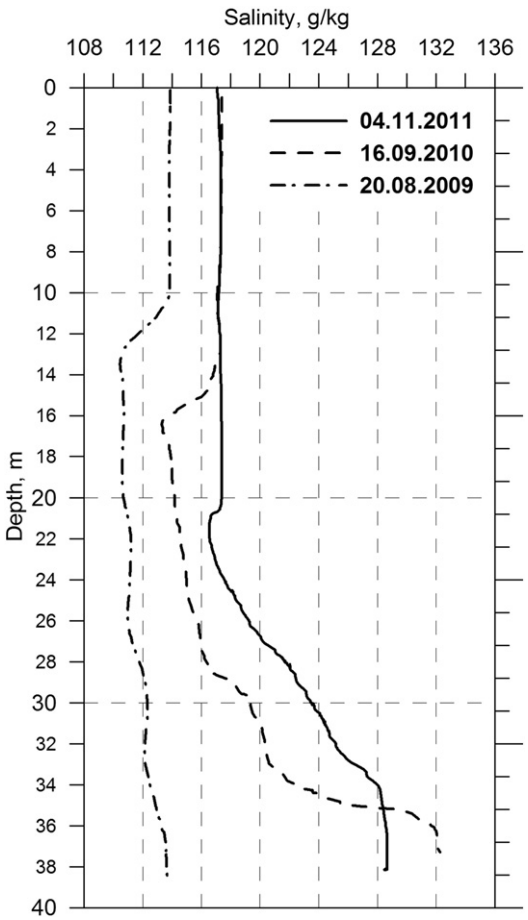

Fig. 6. Vertical profiles of salinity (g/kg), obtained in August, 2009, September, 2010, and November, 2011 at the deepest station on the zonal cross-section.

which is not valid for the conditions of the Aral Sea. For the simulations with non-stratified conditions, we used a constant temperature of 15 °C and a constant salinity of 106 g/kg.

In numerical simulation, we focused on two cases: *unstratified* and *stratified*. Each of these cases involved two experiments with the real and inverted bathymetry. This approach allows investigating the individual contribution from each of the factors in the formation of basin scale circulation.

Accordingly, in total, we performed 4 model experiments: 1) real bathymetry, non-stratified conditions, 2) real bathymetry, stratified conditions, 3) inverted bathymetry, non-stratified conditions, and 4) inverted bathymetry, stratified conditions.

4. Thermohaline structure

Results of the measurements in the western basin of the Aral Sea in August, 2009 are depicted in Fig. 4. The upper mixed layer with temperature about 24 °C and salinity around 113.5 g/kg extended up to 13 m depth in the eastern part of the basin, and 6 to 7 m depth in the western part. Strong seasonal thermocline with vertical gradients of temperature up to 2.2 °C/m separated the upper mixed layer and the intermediate layer with the local minima of salinity and temperature (at 5.5 °C and 110.5 g/kg, respectively). Beneath 25 m depth, there was a bottom layer characterized by temperature inversion and local salinity maximum. Thus, the thermohaline structure of the western basin in August, 2009 exhibited a three-layered pattern with two salinity maxima separated by relatively fresh intermediate layer. Hypothetically, the presence of two salinity maxima resulted from activity of the two forming mechanisms, mentioned above as advective and convective. The reduction of difference between the surface and the bottom salinity values compared with that observed in similar measurements of 2008 (Zavialov, 2009) may indicate weakening of the advective mechanism. Indeed, the eastern basin has shrunk almost completely during the summer of 2009, so the volume of the interbasin exchange and thus the replenishment of the bottom high salinity level must have decreased.

The character of thermohaline structure, observed in the western basin in September, 2010 (Fig. 5), was generally similar to that in August, 2009. Three layers, including surface and bottom local salinity maxima separated by relatively fresh intermediate water, were again seen. The upper mixed layer extended down to 14.5 m depth with average temperature values about 19 °C and average salinity values around 117 g/kg. The steep thermocline with temperature drop as large as of 11 °C over only 3 m of the column was located below upper mixed layer. The core of relatively fresh intermediate layer with temperature values below 7°C and salinity values below 113 g/kg was located under the thermocline. The upper boundary of the bottom layer was located at around 28 m depth, from where salinity values started to increase rapidly downward to the bottom. Also, the bottom salinity maximum was accompanied by typical temperature inversion with temperature growth by up to 4 °C, see also Fig. 6. The difference in salinity values between the surface and the bottom maxima constituted 15 g/kg, which is much higher than that observed in 2009. According to the available satellite data (Soloviov, pers. com.), the volume of water in the eastern basin has grown substantially during the autumn/winter season of 2009/2010, and the exchanges between the basins resumed.

The new results reported above, therefore, appear to be consistent with the hypothesis moved forward in a number of previous studies: the stratification of the western basin depends strongly on the intensity and characteristics of salt exchange between the eastern and the western basins of the sea through the connecting strait. When the eastern basin is either small (situation of 2009) or not as much saltier than the western one, and the salt exchange is reduced, the stratification of the western basin relaxes and tends to take a “two-layered” structure, with only one salinity maximum in the upper layer following intense summer evaporation. The profile of 2009 (Fig. 6) appears to correspond to this situation, followed by restoration of “three-layered” pattern with well-developed salinity maximum at the bottom after the exchange resumed in 2010 (Fig. 6). The bottom salinity decreased again after the exchanges ceased again in 2011.

On the other hand, it has to be kept in mind that there is no data on the salinity of the eastern basin after its replenishment with Amu-Darya water in 2010, and it is not impossible that, at present, it may be actually lower than that in the western basin. Nevertheless, the newly obtained data on the thermohaline structure appear to support the concept of the exchanges with the eastern basin as the principle controller of stratification in the western basin.

5. Water circulation: observations

Some general ideas about nowadays features of water circulation in the Aral Sea could be obtained basing on the analysis of observations as well as model experiments.

Fig. 7 depicts the wind forcing conditions over the western basin during the periods of measurements in the 3 field campaigns. In all 3 cases, the winds blew approximately along the main axis of the basin during the most part of the observations. During the most significant wind events, the wind stress was directed to the south (except the conditions observed in November, 2011). The northerly and northeasterly winds prevail over the Aral Sea basin within most of the year (e.g., Bortnik and Chistyaeva, 1990). Thus, the wind conditions during the measurements were close to the climatic regime.

Fig. 8 (left panel) shows the results of direct measurements of current velocities and directions, as well as sea level variability, conducted in the central part of the western basin in August, 2009. The near-surface current at the eastern slope of the basin has general southward

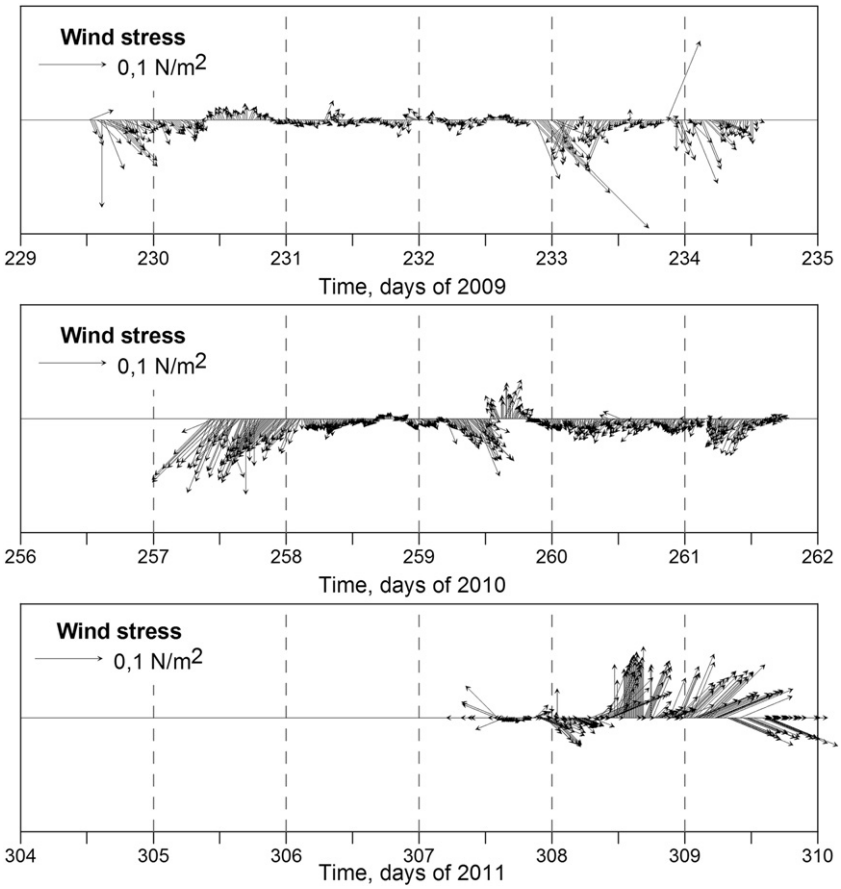

Fig. 7. Vector diagrams of wind stress during the field campaigns of 2009, 2010 and 2011.

alongshore direction during almost the entire period of measurements. The highest velocity values were observed on August 22 after an intense southward wind burst. The near-surface currents at the western slope did not exhibit equally well-defined character, although showing development of northward currents corresponding to northern wind events with some time lag. The sea level rise at the western slope, observed from August 22 to the end of the measurement period, apparently was also caused by the northern wind forcing. The reason of the sharp increase and then change of sign of the current velocity on day 232 is unclear. Hypothetically, that could be a manifestation of seiches, which is believed to be a typical feature of the today's Aral Sea circulation (e.g., Zavialov et al., 2012).

Fig. 8 (right panel) exhibits the result of similar measurements, conducted in the western basin in September, 2010. The atmospheric forcing during the survey generally was more intense than that in the survey of 2009 (Fig. 7). Surface currents at the eastern slope reached the values of 25 cm/s being directed to the south-southwest during the entire measurements period. At the same time, surface currents at the western slope reached values around 45 cm/s with north-northwestward direction. The most significant event of the northerly winds observed in the beginning of the measurements period was accompanied by the sea level rise along the western bank.

Results of current measurements conducted in the western basin during the surveys demonstrate similar features. Despite the relative shortness of observations and some differences in wind forcing for different observation periods, we can conclude that the general directions of water fluxes were quite pronounced, namely, the northward direction for the surface current of the western slope, and southward directions for the surface currents along the eastern shore. This fact was observed in all the 3 surveys (2009, 2010, and 2011, Figs. 8, 9). Similarly, there were predominant directions of the bottom currents at the basin slopes: the current was southward at the western slope, and mainly northward at the eastern slope.

The observed features allow to conclude, that, despite the profound changes in geographical conditions of the region and catastrophic decrease of sea volume, water circulation in the surface layer of the Aral Sea remains anti-cyclonic, while circulation in the bottom layer still retains the cyclonic character.

Some insight into the mechanisms of the basin response to the wind forcing can be obtained through the analysis of time-lagged correlations between the components of wind stress, currents and sea level anomaly. To this end, we analyze here the measurements conducted in September, 2010. We are mainly interested in the basin response to the climatic wind stress, to which the observations of September 2010 were probably the closest proxy. The northern component of the wind stress exhibits positive correlation with northern component of the surface current at the eastern slope for all temporal lags considered (Fig. 10a). In the initial phase of the response to a wind event, the northern component of the surface current at the western slope has positive correlation (maximum $r = 0.52$ for the lag of 6.1 h) with northern component of the wind stress, which then turns to be negative after about 33 h from the beginning (maximum $r = -0.66$ for the lag of 48.5 h, Fig. 10c). At the same time, there is negative correlation between the northern component of the surface current at the eastern slope and sea level anomaly above the western slope with any time lag (Fig. 10b). The northern component of the surface current at the western slope exhibits high positive synchronous correlation ($r = 0.74$ for the lag of 0 h) with the sea level anomaly at the western slope (Fig. 10d). For large lags, this connection transforms to negative and very high ($r = 0.91$ for the lag of 50 h). This transformation of the positive correlations to negative, as

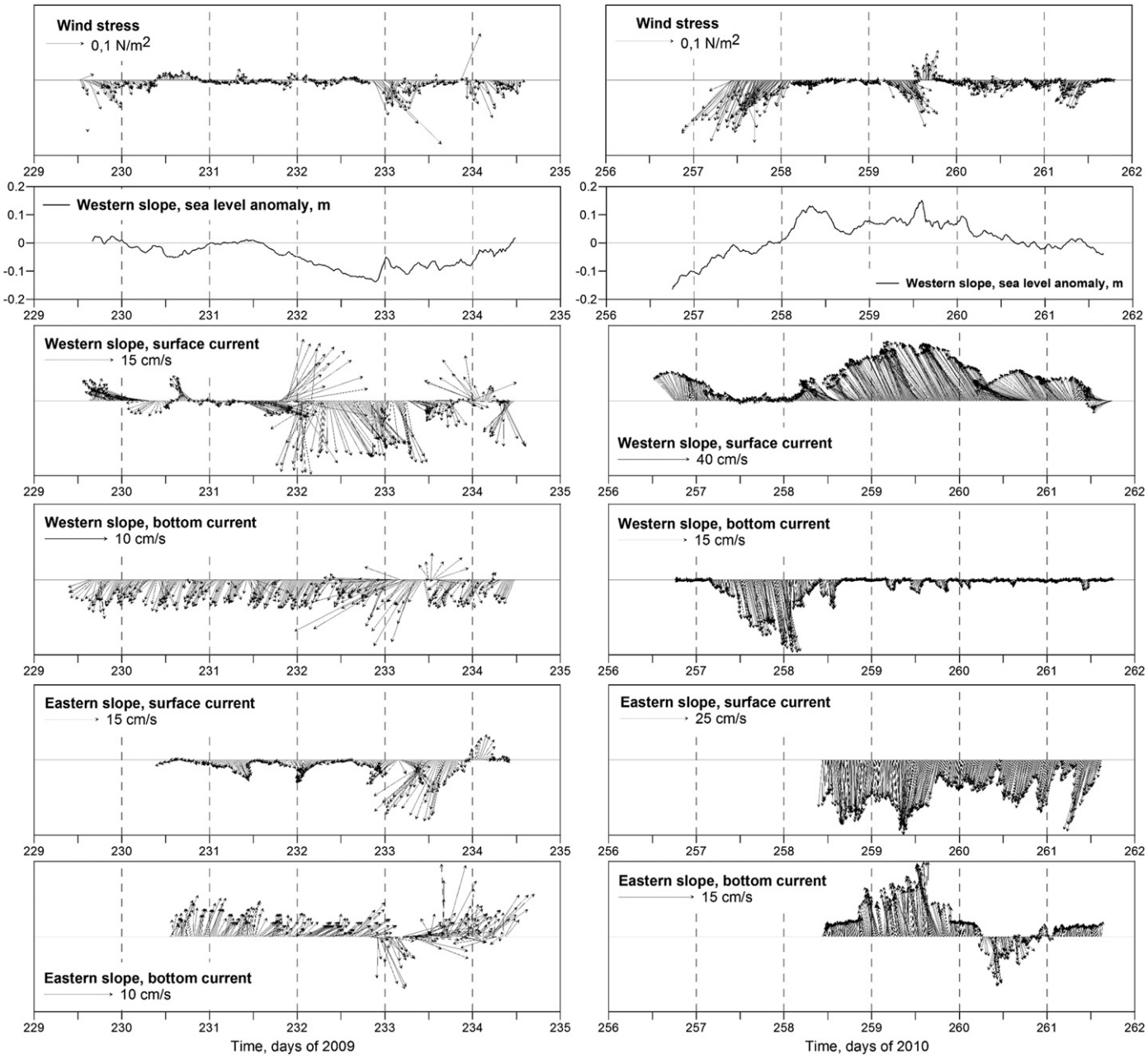

Fig. 8. Current velocities and directions, sea level variability and wind stress variability, obtained from mooring recorders and meteorological station in August, 2009 (left panel) and September, 2010 (right panel). From top to bottom: wind stress vectors (N/m^2), sea level anomaly at station "W" (m), velocity vectors of surface current at station "W" (cm/s), velocity vectors of bottom current at station "W" (cm/s), velocity vectors of surface current at station "E" (cm/s), and velocity vectors of bottom current at station "E" (cm/s).

shown in Fig. 10c and d, points towards the compensative character of the alongshore surface current under the western slope. Indeed, this means that the surface currents at the western bank flow "against" the wind, and reacts not on wind itself but, rather, on the circulation and the level changes across the sea once they are established after some time following wind event. Bottom currents along the slopes of the basin demonstrate the well-pronounced negative correlation ($r = 0.87$) with the maximum at about 40 h time lag (Fig. 10e). Surface currents in the western and eastern parts of the sea show negative correlations with each other for any lag, but the maximum correlation coefficient $r = -0.7$ corresponds to the lag 37.5 h. Together with the measurement data shown in Fig. 8 (right panel) this suggests the existence of anti-cyclonic gyre in the surface layer and cyclonic flow in the bottom.

As mentioned above, the first explanation of the anti-cyclonic character of the Aral Sea's surface circulation was proposed by (Simonov, 1954), who attributed it to the peculiar morphometry of the lake acting together with inhomogeneous wind stress. Presently, the geographical conditions of the Aral Sea, pointed out by A.I. Simonov 59 years ago have changed. The transverse scale of the basin (e.g. about 25 km in 2010) reduced by an order of magnitude, so the inhomogeneous distribution of wind stress over the sea probably no longer has significant influence. However, the peculiar bottom topography of the Aral Sea is still there. The features of the circulation and its response to the wind forcing as observed in the measurements reported in this study are likely to originate from this "asymmetry" in the bottom topography. Shallow eastern areas of the sea respond more energetically to wind forcing, than the deep western areas, so the sea level rise occurs near the western shore during the development of southward along shore current near the eastern coast (Fig. 10b). Accordingly, a northward compensative current develops along the western shore after about 35 h since the wind event (Fig. 10c). The sea level near the western coast begins to decrease (Fig. 10d) and the surface circulation takes the anti-cyclonic character.

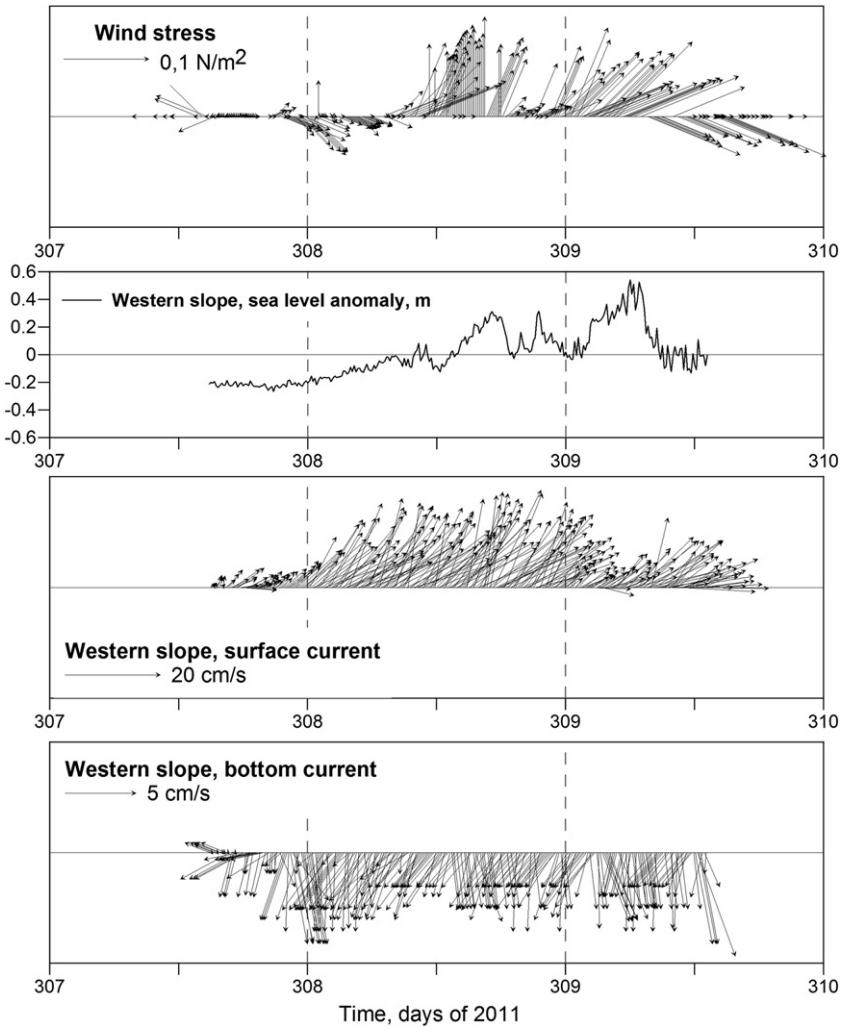

Fig. 9. Data from measurements of November, 2011. From top to bottom: wind stress vectors (N/m^2), sea level anomaly at station "W" (m), velocity vectors of surface current at station "W" (cm/s), and velocity vectors of bottom current at station "W" (cm/s).

Basing on measurements of 2010, the complete period of the establishment of the anti-cylonic flow in the western basin of the Aral Sea following a northerly wind event can be estimated as about 40 h (Fig. 10f). Additional confirmation of this concept of the Aral Sea will be presented below in the modeling section.

6. Water circulation: modeling results

In what follows, firstly, the unstratified case is presented in order to isolate the influence of the bathymetry formation of the circulation. Then, we repeat the experiment for the stratified case to determine the role of water column stratification in Aral's circulation features. We, therefore, conduct two model experiments, one with the "real" bathymetry, and the other one with the bathymetry "inverted" with respect to the long axis of the western basin

6.1. Unstratified case

The results of model experiment using the real bathymetry and the water column of uniform density are shown in Fig. 11 (left panel). The corresponding pattern of the flow at surface exhibits well-developed anticyclonic character of water circulation under the climatic northeasterly winds. The southward surface flow coincides with the relatively shallow parts of the basin, while the deep parts of the basin are mainly occupied by the northward surface flow. The eastern shallow part of the basin is also characterized by the intensification of surface currents.

Imposing of the inverted bathymetry in the case of unstratified basin yields the opposite pattern, as far as the surface layer is concerned (Fig. 11, right panel). In this case, the flow at the surface is organized as a cyclonic gyre with the intensified southward branch along the western coast. Deeper parts of the "inverted" basin along the eastern shore exhibit a less intense northward flow.

The velocity vectors for the bottom layer in this experiment are shown on Fig. 12 (left panel). The general anticyclonic motion occupying the main lobe of the western Aral Sea in the non-stratified case is observed to have the same sense at all depths throughout the water column. The same pattern in the bottom layer is seen for the scenario with the inverted bathymetry, too (Fig. 12, right panel). Hence, bathymetry inversion does not seem to have any significant influence on the circulation character in the bottom layer.

6.2. Stratified case

Introducing a real stratification into the simulation experiments illustrates another important effect. Fig. 13 shows the distribution of velocity vectors in the surface layer in the case of stratified water column. Anticyclonic circulation character of surface circulation still complies with real bathymetry (Fig. 13, left panel) while the cyclonic surface circulation results from the inverted bathymetry

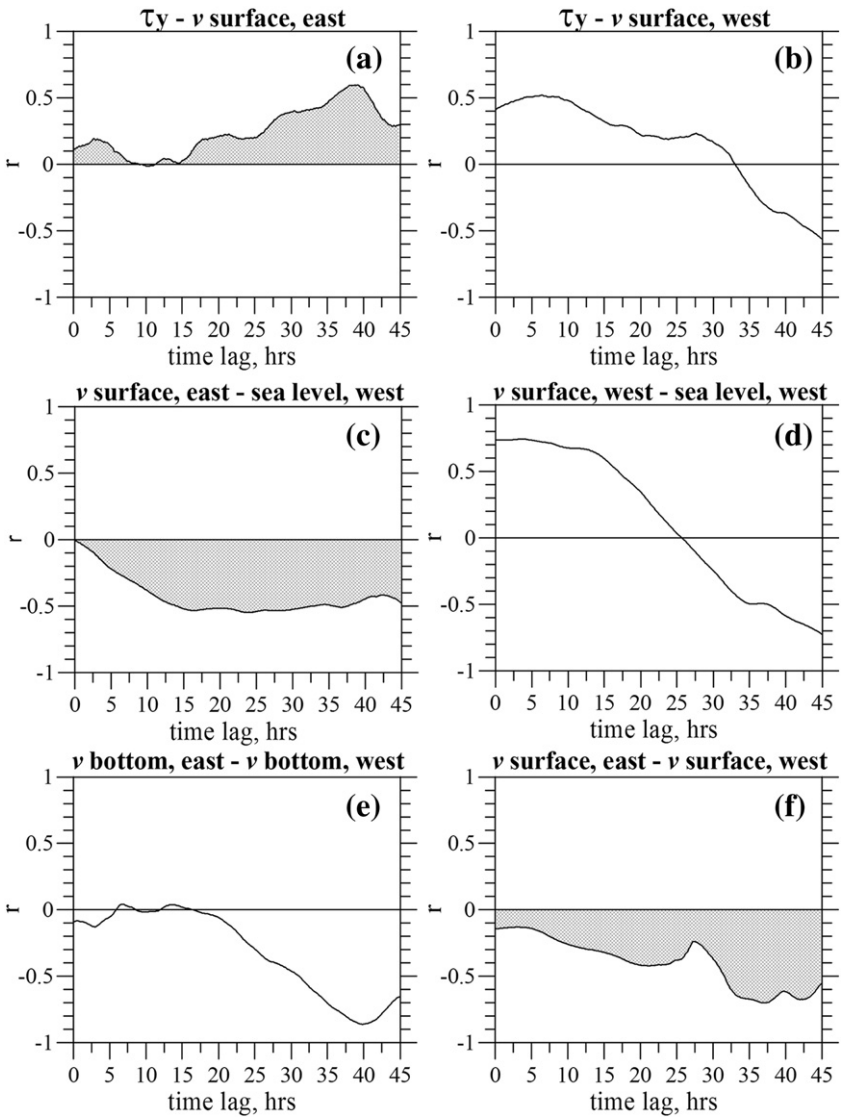

Fig. 10. Lagged correlations between: northern component of the wind stress and northern component of the surface current at station "E" (a), northern component of the surface current at station "E" and the sea level anomaly at station "W" (b), northern component of the wind stress and northern component of the surface current at station "W" (c), northern component of the surface current at station "W" and the sea level anomaly at station "W" (d), northern components of the bottom currents at stations "E" and "W" (e), northern components of the surface currents at stations "E" and "W" (f).

(Fig. 13, right panel). A constant and uniform NE wind was used as a forcing factor in both cases. Therefore, in the stratified case, the bathymetry pattern still constitutes the dominant role in the formation of circulation character at the surface. The bathymetry inversion alone led to the change of the circulation sign to the opposite under the otherwise constant conditions, no matter whether the column was stratified or not. However, it should be pointed out, that the velocity field in the stratified case is more complex than that for the non-stratified scenario. In the stratified case, the circulation pattern includes smaller, sub-basin scale gyres (anti-cyclonic for the real bathymetry and cyclonic for the inverted bathymetry) occupying the central part of the basin (Fig. 13).

On the other hand, the introduction of stratification does affect significantly the circulation character in the bottom layer of the basin, causing development of a cyclonic gyre (Fig. 14). The dominance of cyclonic vorticity in the bottom layer was observed both in cases of the real and inverted bathymetries and depended only on the presence of stratification. In the case of real bathymetry, a clockwise gyre is observed in the central part of the western trench. In this region, the sign of the circulation does not change from surface to bottom (Figs. 13, 14). In addition, there are two well-developed smaller eddies in the northern and southern vicinities of the central gyre (Figs. 13, 14). These smaller gyres are anti-cyclonic in the upper layer and cyclonic in the lower layer. This "two-layered" character of the water circulation is apparently caused by the presence of stratification. The location of the bottom cyclonic gyres is likely to be sensible to the wind direction. In situ observations with better coverage in space and time will help to clarify the question in the future.

7. Conclusions

1. During the study period, the hydrological structure of the Aral's western basin in autumn exhibited a three-layered pattern with two local salinity maxima, separated by a fresher intermediate layer. As hypothesized in previous publications (e.g. Zavialov, 2005; Zavialov et al., 2012), the observed structure resulted from combined action of two forming mechanisms, referred to as "convective" and "advective".
2. The latter, connected with the water exchange between the western and the eastern basins of the Large Aral Sea, is subject to significant interannual changes. Indeed, in the summer of 2009, when the eastern basin had dried almost completely and the interbasin exchange

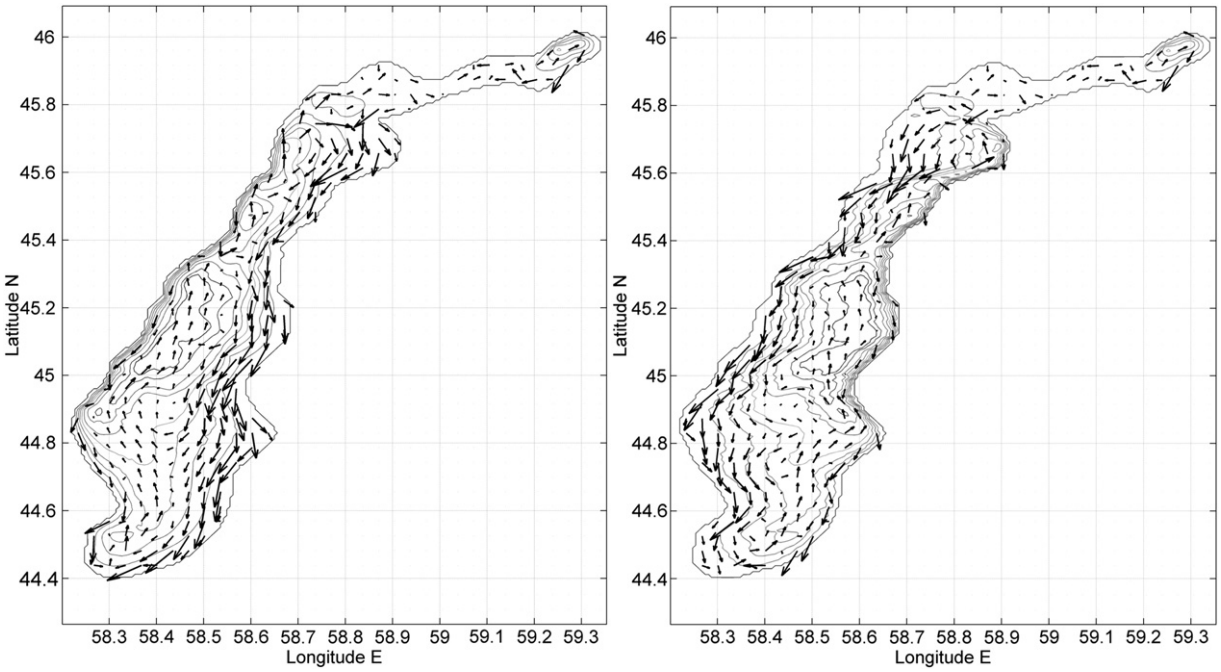

Fig. 11. Simulated surface circulation in case of non-stratified basin: real bathymetry (left panel), inverted bathymetry (right panel).

had practically ceased, the salinity values at the surface and in the bottom were close to each other. Subsequently, the intensity of the interbasin exchanges increased again, and in the autumn of 2011, the difference in salinity between the surface and the bottom layers attained high values around 11 g/kg, while the relatively fresh intermediate layer remained between the two salinity maxima.

3. Despite the profound changes in geographical and hydrological conditions of the lake, water circulation in the deep western basin still retains its peculiar character, typical for the Aral Sea in its pre-desiccation state. According to direct observations, water circulation in the surface layer has anti-cyclonic character, while circulation in the bottom layer is more complex but generally has cyclonic sign under the predominant northerly winds.
4. We implemented a series of numerical model experiments with innovative approach involving the "inverted" bathymetry of the lake along with the true one. These model experiments, as well as the data analyses, helped to elucidate the origins of the anti-cyclonic circulation establishment in the surface layer of the lake: the main reason for this feature is the "asymmetric" bathymetry with broad shallow area along the eastern coast and relatively steep and deep

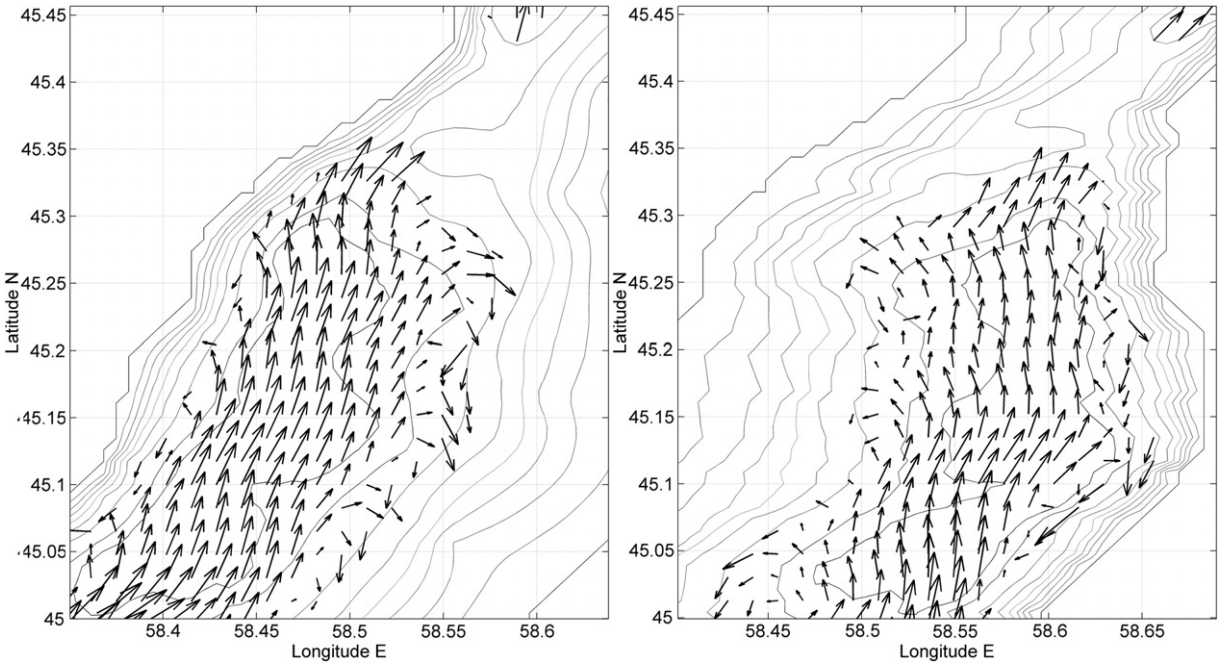

Fig. 12. Simulated water circulation in the bottom layer (29 m depth) in case of non-stratified basin: real bathymetry (left panel) and inverted bathymetry (right panel).

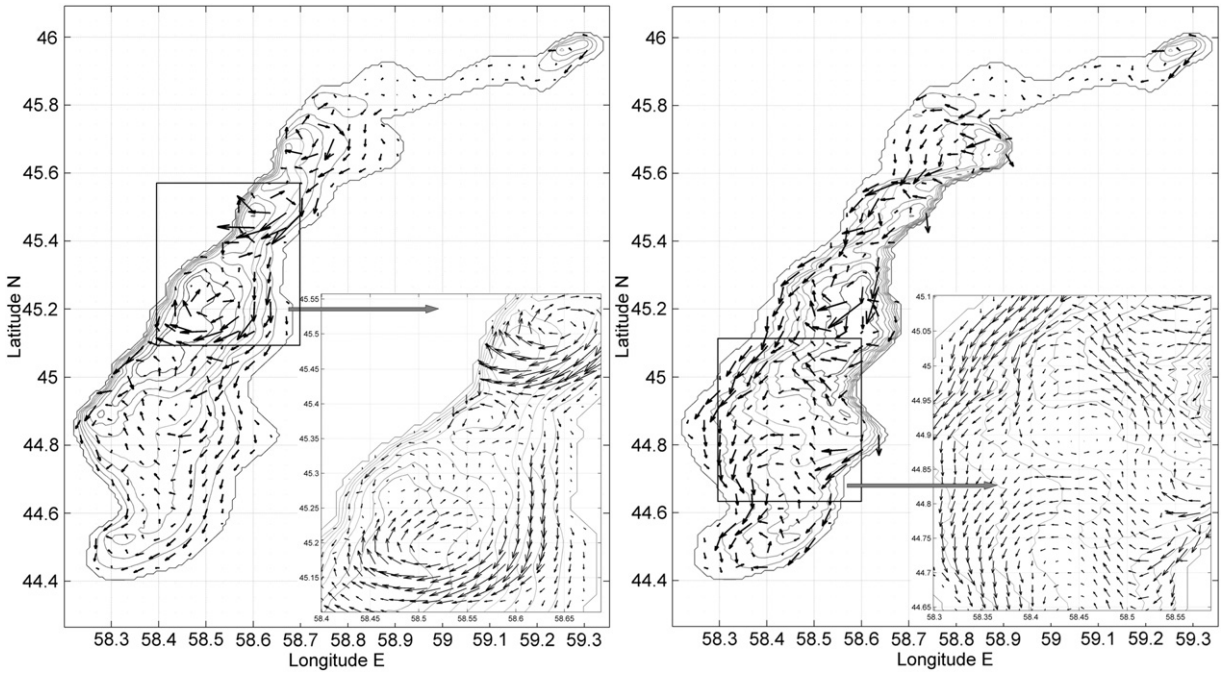

Fig. 13. Simulated surface circulation in the western basin in case of stratified basin: real bathymetry (left panel), inverted bathymetry (right panel).

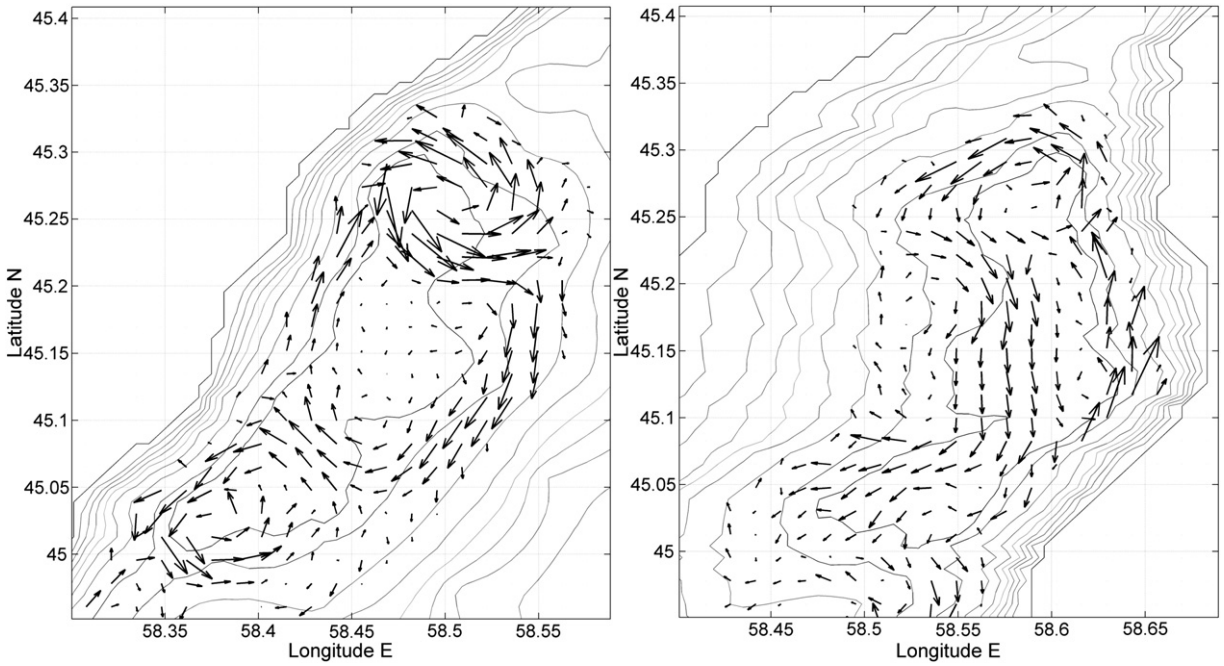

Fig. 14. Simulated water circulation in the bottom layer (29 m depth) in case of stratified basin in dependence of bathymetry: real bathymetry (left panel) and inverted bathymetry (right panel).

western part. Simulation experiments demonstrated clearly that surface circulation switches to the opposite sign as soon as the bathymetry is inverted with respect to the longitudinal axis of the basin.

5. According to modeling results, development of the circulation in the bottom layer of the basin is intimately connected with the basin stratification and does not directly depend on the bathymetry.

Acknowledgments

The authors gratefully acknowledge invaluable assistance of their collaborators and colleagues from Tashkent Institute of Geology and Geophysics, as well as the support received from EU FP7 Project CLIMSEAS (IRSES-2009 N.247512), U.S. Civil Research and Development Foundation (grant RUG1-2968-MO-10), and the Russian Ministry of Education and Science.

References

Beletsky, D., Saylor, J.H., Schwab, D.J., 1999. Mean circulation in the Great Lakes. J. Great Lakes Res. 25 (1), 78–93.

Beletsky, D., Schwab, D., McCormick, M., 2006. Modeling the 1998–2003 summer circulation and thermal structure in Lake Michigan. J. Geophys. Res. 111 (C10010).

Berg, L.S., 1908. Aral Sea. An Attempt of Physical Geographic Description. Izvestiya Turkestanskogo Otdeleniya. , 5. Russian Geographic Society, St. Petersburg 9 (580 pp. (in Russian)).
Bortnik, V.N., Chistyaeva, S.P., 1990. Hydrometeorology and Hydrochemistry of the USSR Seas. The Aral Sea, Vol. VII. Gidrometeoizdat, Leningrad (196 pp. (in Russian)).
Gertman, I., Zavialov, P.O., 2011. New equation of state for Aral Sea water. Oceanology 51, 367–369 (in Russian).
Ginzburg, A.I., Kostianoy, A.G., Sheremet, N.A., 2002. Thermal regime of the Aral Sea at present time (1982–2000) based on satellite data. Issled. Zemli iz Kosmosa 4, 62–69 (in Russian).
Hasselman, S., 1988. The WAM model — a third generation ocean wave prediction model. J. Phys. Oceanogr. 18, 1775–1810.
Kosarev, A.N., 1975. Hydrology of Caspian Sea and Aral Sea. Moscow State University, Moscow (272 pp. (in Russian)).
Marti, C.L., Imberger, J., 2008. Exchange between littoral and pelagic waters in a stratified lake due to wind-induced motions: Lake Kinneret, Israel. Hydrobiologia 603, 25–51.
Mellor, G.L., 1992. User's guide for a three-dimensional, primitive equation, numerical ocean model. Progress in Atmospheric and Oceanic Sciences. Princeton University, Princeton (35 pp.).
Pickett, R.L., Bermick, S., 1977. Observed resultant circulation of Lake Ontario. Limnol. Oceanogr. 22, 1071–1076.
Roget, E., Zavialov, P.O., Khan, V.M., Muniz, M.A., 2009. Geodynamical processes in the channel connecting the two lobes of the Large Aral Sea. Hydrol. Earth Syst. Sci. 13, 2265–2271.
Rueda, F.J., Schladow, S.G., Monismith, S.G., Stacey, M.T., 2005. On the effects of topography on wind and the generation of currents in a large multi-basin lake. Hydrobiologia 532, 139–151.
Schwab, D.J., Beletsky, D., 2003. Relative effects of wind stress curl, topography, and stratification on large-scale circulation in Lake Michigan. J. Geophys. Res. 108, 3044.
Shimizu, K., Imberger, J., Kumagai, M., 2007. Horizontal structure and excitation of primary motions in a strongly stratified lake. Limnol. Oceanogr. 52 (6), 2641–2655.
Shtokman, V.B., 1953. Impact of bottom topography and transversal wind variability to horizontal circulation in the shallow sea or the water storage basin. Meteorol. Gidrol. 8, 16–22 (in Russian).
Simonov, A.I., 1954. On origins of anticyclonic circulation of the Aral Sea waters. Meteorol. Gidrol. 2, 50–52 (in Russian).
Simonov, A.I., 1962. Origin of relatively high-salt waters in the western trench of the Aral Sea. Tr. GOIN 68, 103–117 (in Russian).
Strub, P.T., Powell, T.M., 1986. Wind-driven surface transport in stratified closed basins: direct versus residual circulations. J. Geophys. Res. 91, 8497–8508.
Zavialov, P.O., 2005. Physical Oceanography of the Dying Aral Sea. Springer-Verlag/Praxis, Chichester, UK (158 pp.).
Zavialov, P.O., 2009. Physical oceanography of the Large Aral Sea. In: Kostianoy, A.G., Kosarev, A.N. (Eds.), Aral Sea Environment. Hdb Env Chem. Springer-Verlag, pp. 123–146.
Zavialov, P.O., Arashkevich, E.G., Bastida, I., Ginzburg, A.I., Dikarev, S.N., Zhitina, L.S., Izhitskiy, A.S., Ishniyazov, D.P., Kostianoy, A.G., Kravtsova, V.I., Kudyshkin, T.V., Kurbaniyazov, A.K., Ni, A.A., Nikishina, A.B., Petrov, M.A., Sazhin, A.F., Sapozhnikov, P.V., Soloviov, D.M., Khan, V.M., Sheremet, N.A., 2012. The Large Aral Sea in the Beginning of Century 21: Physics, Biology. Chemistry. Nauka, Moscow (229 pp. (in Russian)).
Zhdanko, S.M., 1940. Currents in the Aral Sea. Meteorol. Gidrol. 1–2, 78–82 (in Russian).